



UNIVERSIDADE ESTADUAL DE CAMPINAS
SISTEMA DE BIBLIOTECAS DA UNICAMP
REPOSITÓRIO DA PRODUÇÃO CIENTÍFICA E INTELLECTUAL DA UNICAMP

Versão do arquivo anexado / Version of attached file:

Versão do Editor / Published Version

Mais informações no site da editora / Further information on publisher's website:

<https://www.osapublishing.org/ome/abstract.cfm?uri=ome-7-7-2528>

DOI: 10.1364/OME.7.002528

Direitos autorais / Publisher's copyright statement:

©2017 by Optical Society of America. All rights reserved.

DIRETORIA DE TRATAMENTO DA INFORMAÇÃO

Cidade Universitária Zeferino Vaz Barão Geraldo

CEP 13083-970 – Campinas SP

Fone: (19) 3521-6493

<http://www.repositorio.unicamp.br>



Controlled stacking of graphene monolayer saturable absorbers for ultrashort pulse generation in erbium-doped fiber lasers

HENRIQUE G. ROSA,¹ JUAN A. CASTAÑEDA,² CARLOS H. BRITO CRUZ,² LÁZARO A. PADILHA,² JOSÉ C. V. GOMES,¹ EUNÉZIO A. THOROH DE SOUZA,^{3,*} AND HUGO L. FRAGNITO³

¹Centre for Advanced 2D Materials and Graphene Research Centre, National University of Singapore, Singapore 117542, Singapore

²Instituto de Física “Gleb Wataghin”, Universidade Estadual de Campinas, UNICAMP, P.O. Box 6165, 13083-859 Campinas, Sao Paulo, Brazil

³MackGraphe, Graphene and Nanomaterials Research Centre, Mackenzie Presbyterian University, São Paulo, Brazil.

*thoroh@mackenzie.br

Abstract: Stacked chemical-vapour deposited (CVD) graphene monolayer samples were fabricated and applied as saturable absorbers in erbium-doped fiber laser (EDFL). Transient absorption experiments show that at the saturation absorption regime, and regardless the number of stacked layers (from 1 to 5 layers), samples present 1 ps recovery time. Pulses with duration from 0.60 to 1.17 ps were generated in an EDFL, depending on the number of graphene layers (i.e., the linear optical absorption) used. The results show that it is possible to increase the linear optical absorption of a graphene stacking without affecting its nonlinear optical behavior and ultrafast response time. Therefore, by stacking individual CVD-monolayer graphene samples it is possible to control the optical properties in graphene-based EDFLs and simultaneously tune their ultra-short pulse generation.

© 2017 Optical Society of America

OCIS codes: (160.4236) Nanomaterials; (190.7110) Ultrafast nonlinear optics; (320.7150) Ultrafast spectroscopy; (060.3510) Lasers, fiber; (140.4050) Mode-locked lasers.

References

1. A. H. Castro Neto, F. Guinea, N. M. R. Peres, K. S. Novoselov, and A. K. Geim, “The electronic properties of graphene,” *Rev. Mod. Phys.* **81**(1), 109–162 (2009).
2. F. Bonaccorso, Z. Sun, T. Hasan, and A. C. Ferrari, “Graphene photonics and optoelectronics,” *Nat. Photonics* **4**(9), 611–622 (2010).
3. F. Xia and P. Avouris, “Graphene Nanophotonics,” *IEEE Photonics J.* **3**(2), 293–295 (2011).
4. D. Popa, Z. Sun, F. Torrisi, T. Hasan, F. Wang, and A. C. Ferrari, “Sub 200 fs pulse generation from a graphene mode-locked fiber laser,” *Appl. Phys. Lett.* **97**(20), 2010–2012 (2010).
5. G. Sobon, J. Sotor, and K. M. Abramski, “All-polarization maintaining femtosecond Er-doped fiber laser mode-locked by graphene saturable absorber,” *Laser Phys. Lett.* **9**(8), 581–586 (2012).
6. Y. Meng, S. Zhang, X. Li, H. Li, J. Du, and Y. Hao, “Multiple-soliton dynamic patterns in a graphene mode-locked fiber laser,” *Opt. Express* **20**(6), 6685–6692 (2012).
7. L. Chen, M. Zhang, C. Zhou, Y. Cai, L. Ren, and Z. Zhang, “Ultra-low repetition rate linear-cavity erbium-doped fibre laser modelocked with semiconductor saturable absorber mirror,” *Electron. Lett.* **45**(14), 731–733 (2009).
8. Y.-H. Lin, C.-Y. Yang, J.-H. Liou, C.-P. Yu, and G.-R. Lin, “Using graphene nano-particle embedded in photonic crystal fiber for evanescent wave mode-locking of fiber laser,” *Opt. Express* **21**(14), 16763–16776 (2013).
9. A. Castellanos-Gomez, M. Buscema, R. Molenaar, V. Singh, L. Janssen, H. S. J. van der Zant, and G. a Steele, “Deterministic transfer of two-dimensional materials by all-dry viscoelastic stamping,” *2D Mater.* **1**, 11002 (2014).
10. H. G. Rosa, J. C. V. Gomes, and E. A. T. de Souza, “Transfer of an exfoliated monolayer graphene flake onto an optical fiber end face for erbium-doped fiber laser mode-locking,” *2D Mater.* **2**, 31001 (2015).
11. P. L. Huang, S.-C. Lin, C.-Y. Yeh, H.-H. Kuo, S.-H. Huang, G.-R. Lin, L.-J. Li, C.-Y. Su, and W.-H. Cheng, “Stable mode-locked fiber laser based on CVD fabricated graphene saturable absorber,” *Opt. Express* **20**(3), 2460–2465 (2012).

12. Q. Bao, H. Zhang, Y. Wang, Z. Ni, Y. Yan, Z. X. Shen, K. P. Loh, and D. Y. Tang, "Atomic-Layer Graphene as a Saturable Absorber for Ultrafast Pulsed Lasers-support info," *Adv. Funct. Mater.* **19**(19), 3077–3083 (2009).
13. J. D. Zapata, D. Steinberg, L. A. M. Saito, R. E. P. de Oliveira, A. M. Cárdenas, and E. A. T. de Souza, "Efficient graphene saturable absorbers on D-shaped optical fiber for ultrashort pulse generation," *Sci. Rep.* **6**(1), 20644 (2016).
14. Y. Hernandez, V. Nicolosi, M. Lotya, F. M. Blighe, Z. Sun, S. De, I. T. McGovern, B. Holland, M. Byrne, Y. K. Gun'Ko, J. J. Boland, P. Niraj, G. Duesberg, S. Krishnamurthy, R. Goodhue, J. Hutchison, V. Scardaci, A. C. Ferrari, and J. N. Coleman, "High-yield production of graphene by liquid-phase exfoliation of graphite," *Nat. Nanotechnol.* **3**(9), 563–568 (2008).
15. J. W. Suk, A. Kitt, C. W. Magnuson, Y. Hao, S. Ahmed, J. An, A. K. Swan, B. B. Goldberg, and R. S. Ruoff, "Transfer of CVD-grown monolayer graphene onto arbitrary substrates," *ACS Nano* **5**(9), 6916–6924 (2011).
16. Y. Wang, S. W. Tong, X. F. Xu, B. Özyilmaz, and K. P. Loh, "Interface engineering of layer-by-layer stacked graphene anodes for high-performance organic solar cells," *Adv. Mater.* **23**(13), 1514–1518 (2011).
17. G. Zheng, Y. Chen, H. Huang, C. Zhao, S. Lu, S. Chen, H. Zhang, and S. Wen, "Improved transfer quality of CVD-grown graphene by ultrasonic processing of target substrates: applications for ultra-fast laser photonics," *ACS Appl. Mater. Interfaces* **5**(20), 10288–10293 (2013).
18. Y. He, W. F. Chen, W. B. Yu, G. Ouyang, and G. W. Yang, "Anomalous interface adhesion of graphene membranes," *Sci. Rep.* **3**(1), 2660 (2013).
19. G. D. Kwon, E. Moyon, Y. J. Lee, Y. W. Kim, S. H. Baik, and D. Pribat, "Influence of the copper substrate roughness on the electrical quality of graphene," *Mater. Res. Express* **4**(1), 015604 (2017).
20. H. Wang, J. H. Strait, P. A. George, S. Shivaraman, V. B. Shields, M. Chandrashekhar, J. Hwang, F. Rana, M. G. Spencer, C. S. Ruiz-Vargas, and J. Park, "Ultrafast relaxation dynamics of hot optical phonons in graphene," *Appl. Phys. Lett.* **96**(8), 081917 (2010).
21. G. Xing, H. Guo, X. Zhang, T. C. Sum, and C. H. A. Huan, "The Physics of ultrafast saturable absorption in graphene," *Opt. Express* **18**(5), 4564–4573 (2010).
22. F. X. Kurtner, J. A. Der Au, and U. Keller, "Mode-locking with slow and fast saturable absorbers-what's the difference?" *IEEE J. Sel. Top. Quantum Electron.* **4**(2), 159–168 (1998).
23. L. E. E. Nelson, D. J. J. Jones, K. Tamura, H. Haus, and E. P. P. Ippen, "Ultrashort-pulse fiber ring lasers," *Appl. Phys. B Lasers Opt.* **65**(2), 277–294 (1997).
24. H. G. Rosa and E. A. De Souza, "Bandwidth optimization of a Carbon Nanotubes mode-locked Erbium-doped fiber laser," *Opt. Fiber Technol.* **18**(2), 59–62 (2012).
25. W. D. Tan, C. Y. Su, R. J. Knize, G. Q. Xie, L. J. Li, and D. Y. Tang, "Mode locking of ceramic Nd:yttrium aluminum garnet with graphene as a saturable absorber," *Appl. Phys. Lett.* **96**(3), 031106 (2010).
26. G. Sobon, J. Sotor, and K. M. Abramski, "Passive harmonic mode-locking in Er-doped fiber laser based on graphene saturable absorber with repetition rates scalable to 2.22 GHz," *Appl. Phys. Lett.* **100**(16), 161109 (2012).

1. Introduction

Mode-locked Erbium-doped fiber lasers (EDFL) have been of great interest for science and industry, with potential applications in areas such as metrology and optical communications, because of the ability to generate broadband and ultrashort infrared laser pulses with high pulse-to-pulse stability.

In this context, graphene has emerged as one of the most promising candidates as saturable absorbers for EDFL due to its broadband and high absorption coefficient [1–3], moreover being of relatively simple fabrication and cost-effective. Pulses as short as 170 fs have been reported in graphene-based mode-locked EDFL [4]. Recently, mode-locked EDFL were demonstrated in many different laser cavity configurations [5–7], and with different graphene saturable absorbers incorporation methods, including graphene-filled photonic crystal fibers [8], exfoliated [9,10] and CVD graphene [11,12] transferred to the tip of an optical fiber, and CVD graphene transferred to the polished face of an D-fiber [13].

Graphene saturable absorbers have been produced, mainly, by micromechanical exfoliation [9,10], chemical exfoliation [14], and CVD synthesis [15]. In micromechanical exfoliation, samples with high structural quality single crystal flakes, low defects, number of layers easier to characterize by Raman spectroscopy and atomic force microscopy, smaller areas (typically hundreds of μm^2) are obtained, while with CVD synthesis larger area samples can be grown (larger than $\sim 10\text{ cm}^2$). However, CVD samples present a higher defect level and, except for 1 and 2 layers, it is difficult to control the number of graphene layers during fabrication. For optics and optical fiber applications, it is desirable to use graphene samples

combining the best of both methods, with controlled number of layers and larger areas, making their manipulation and fabrication easier.

In this paper, CVD graphene monolayer samples are used to fabricate multilayer graphene, using a combined method for transferring and stacking graphene monolayers, and we demonstrate the application of these stacked graphene samples as saturable absorbers in EDFL. The effects of the number of graphene layers on its total optical absorption and how it affects the performance of the fiber laser system were studied using transient absorption and ultrashort pulse generation experiments, both at 1550 nm. We observed that stacked CVD monolayer graphene samples behave like independent monolayer samples at saturation absorption regime, thus making it possible to control the optical properties of the samples without affecting their ultrafast response. Regardless of the number of layers, graphene stacked samples display 1.0 ps absorption recovery time. Pulses with duration ranging from 0.60 ps to 1.17 ps were generated, and pulse duration dependence on the number of layers was investigated.

2. Samples fabrication

Individual CVD graphene monolayer samples used in this work are commercial-grade graphene grown onto copper foils. Initially, to test the samples quality, such as homogeneity and number of layers, samples were transferred via conventional wet-transfer process [15] onto a clean silica substrate and were characterized by Raman spectroscopy and optical linear transmittance. Those tests revealed a very low defect level and an intensity ratio between G and 2D bands equal to 0.25, demonstrating that the samples are indeed graphene monolayer (see Appendix A).

For our studies, it is essential that the saturable absorbers have a well-defined number of layers. However, during graphene fabrication via CVD, it is difficult to obtain few-layer graphene samples with controlled number of layers. To overcome this limitation, and obtain multi-layer graphene samples with exactly controlled number of layers, several monolayer samples were stacked for the post-fabrication of saturable absorber samples, until the desired number of layers was reached. To achieve this, two methods for graphene transferring and stacking were combined: the method for stacking graphene monolayer samples [16], as can be seen in Fig. 1, and the improved substrate cleaning wet transfer method [17].

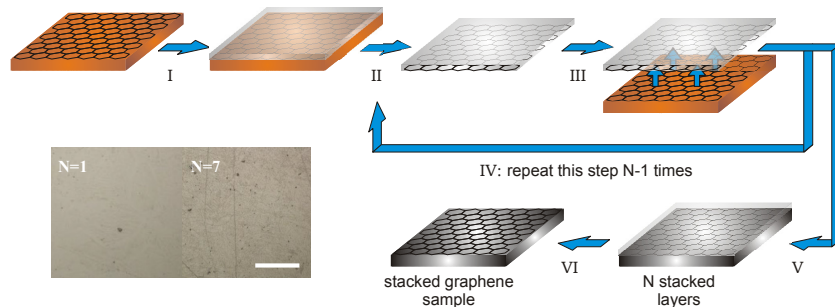


Fig. 1. Transfer and stacking process for fabrication of samples with N stacked CVD graphene monolayer layers. Conventional wet-transfer process is identical to the stacking process by skipping step IV. Inset (bottom-left): optical microscopy images for $N = 1$ and $N = 7$ (scale bar = 500 μm).

The schematic diagram for stacking CVD graphene monolayers is similar to the process for conventional wet transfer, however in the stacking process a polymethyl methacrylate (PMMA) coating for graphene protection is used only once, in the first layer, so in-between layers there is minimal chemical residues and contaminants. In step I, the graphene monolayer is prepared for the transfer process, and in step II it receives a protective coating of PMMA (spin-coated, 300 nm thick). In step III, copper is chemically removed and, after

being rinsed in deionized water baths, the floating PMMA-graphene film is scooped by a clean, as fabricated, sample of CVD monolayer graphene on copper. After each layer of graphene is scooped, the sample goes through a thermal treatment at 100°C for 1 hour. The procedure goes back to step II for copper chemical removal. This iteration (step IV) must be repeated $N-1$ times until the desired number of layers, N , is reached. Then the PMMA-graphene sample (N layers) is scooped by the final substrate (glass substrate and/or polished end-face of optical fiber) in step V. At the end of the process, the PMMA layer is removed in acetone bath (step VI).

With this process, stacked CVD graphene monolayer samples can be transferred to several desired substrates with a controlled number of layers, and with no chemical residues in-between layers. In this work, two sets of samples were fabricated in identical procedures. In one set, graphene samples with 1 to 5 layers were transferred to silica substrates and, in the second, graphene samples with 1 to 7 layers were transferred to single-mode optical fiber connectors. Samples on silica substrates were used for characterization with Raman spectroscopy, linear transmission spectroscopy and ultrafast electron relaxation measurements, while the samples on optical fiber connectors were used as saturable absorbers for application EDFL ultrashort pulse generation. Both substrates, silica slab and the polished end-face of optical fiber, were first cleaned in ultrasonic baths [17].

It is known that graphene-substrate adhesion energy decreases with the number of layers [18]. However, here the transfer process is executed monolayer by monolayer, though ensuring increased adhesion between graphene/substrate and graphene/graphene interfaces, and no adhesion issue was observed.

The optical linear transmittance of the stacked graphene samples was investigated with continuous-wave, low power, 1550 nm laser. The optical linear absorption of the stacked monolayer samples at 1550 nm is approximately $2.15 \pm 0.02\%$ per layer (see Appendix A), close to the expected theoretical value of 2.3% per layer for visible and near-infrared light [16]. This result shows that the stacking of several graphene monolayer samples does not compromise the linear optical properties of individual layers.

To verify whether the stacking process interferes on the density of defects, Raman spectroscopy characterization was performed. The results show that the intensity ratio between D and G bands is kept to a maximum of 0.042, indicating that the process of stacking graphene monolayer does not contribute to an increased relative number of defects in the final samples (see Appendix A).

The roughness of the resulting samples was also measured, by atomic force microscopy, and the RMS roughness increased with the number of layers, ranging from 3.7 nm ($N = 1$) to 19.3 nm ($N = 7$) (see Appendix A). Since graphene is known to conform itself onto its substrate's topology, these RMS roughness values are in agreement with typical values for roughness of copper foils used for CVD growth [19].

3. Ultrafast optical spectroscopy

To further investigate how the stacking process influences the interconnection between adjacent graphene monolayers, we have performed ultrafast transient absorption experiment for samples with the number of graphene monolayers ranging from 1 to 5 layers. The optical excitation source is composed by an amplified Ti:Sapphire laser at 800 nm, delivering 100 fs pulses at 1 kHz repetition rate, and the probe has been chosen at 1550nm (refer to Appendix B for experimental details on the ultrafast spectroscopy).

Figure 2 shows the normalized maximum differential transmittance, as a function of pump intensity and delay time between pump and probe pulses.

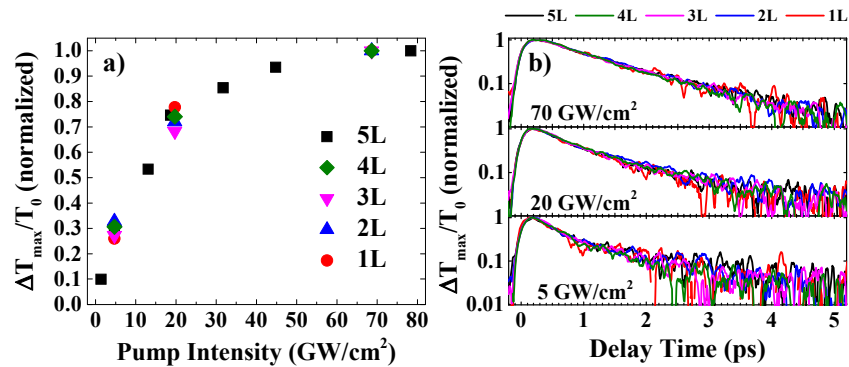


Fig. 2. (a) Maximum differential transmittance as a function of pump intensity and (b) transient absorption characterization, for samples 1 to 5 stacked graphene monolayers. All the samples exhibit the same ultrafast relaxation dynamics at the three pump intensities. The recovery time is ~ 1 ps.

It can be observed from Fig. 2 that samples reached their absorption saturation at the same pump intensity level. It is important to mention that $\Delta T_{\max}/T_0$ scales linearly with the number of graphene layers for each sample (absorption scales linearly with number of layers), therefore the modulation depth of the ultrafast spectroscopy measurement can be increased with the number of stacked graphene monolayers.

The transient absorption, for all five samples, was measured at three different pump intensities (5, 20 and 70 GW/cm^2). As shown in Fig. 2(b), the electron dynamics becomes slower as the intensity is increased to the saturation regime, which may be due to saturation of optical-phonon relaxation channel, reducing the electron phonon interaction rate [20]. Meanwhile, for each pump intensity, the ultrafast relaxation dynamics is not dependent on the number of stacked graphene monolayers. The absorption recovers with a characteristic time of ~ 1 ps. An interconnection between adjacent monolayers would introduce other decay channels in the electronic dynamics, reducing the effective lifetime. The lack of sample dependence of the electron dynamics indicates that these stacked samples are constituted of weakly-coupled (or even uncoupled) monolayers, confirming the findings from the Raman spectroscopy characterization (see Appendix A).

All those results show that, by changing the number of monolayers, it is possible to control the samples optical properties (linear absorption with/without excitation) without changing the absorption properties and the ultrafast absorption relaxation dynamics. Our samples show a saturation intensity in the order of 10 GW/cm^2 , which is in agreement with previously published results for graphene samples pumped by high power 800 nm pulses [21].

4. Ultrashort pulse generation

An EDFL was set up to study the ultrashort pulse generation using the stacked graphene monolayer samples as saturable absorbers (refer to Appendix C for details on the fiber laser experimental setup).

For comparison between laser pulse duration generated with different samples, output power during mode-locking operation was kept constant at 3 mW. At this power level, single-pulse laser operation is achieved and no harmonic mode-locking is observed. The fiber laser performance was measured by an optical spectrum analyzer (0.06 nm resolution) and an intensity autocorrelator (0.01 ps resolution). The pulse duration and bandwidth of the generated solitonic output pulses with the absorber samples having from 1 to 7 layers are shown in Fig. 3.

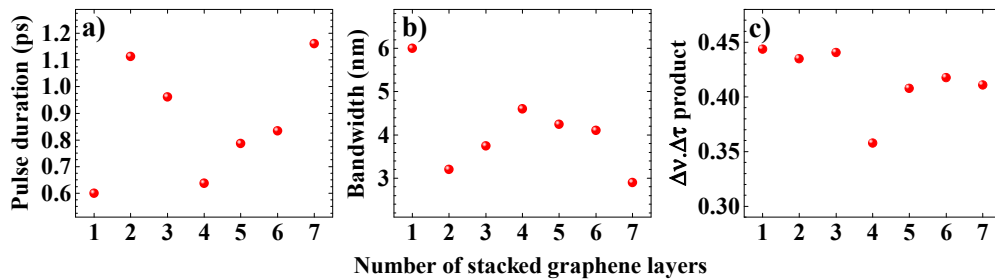


Fig. 3. Full width at half-maximum (a) pulse duration and (b) bandwidth as a function of the number of stacked layers; (c) time-bandwidth product.

As it can be seen in Fig. 3(a), the pulse duration seems to follow a different trend for the case of $N = 1$ and $N = 2\sim 7$ layers, with similar behavior being also observed for the bandwidth in Fig. 3(b). By just considering results for samples with 2 to 7 layers, the pulse duration is shortened from 1.11 ps for 2 layers to a minimum of 0.64 ps for 4 layers, and then is stretched up to 1.16 ps for 7 layers. Opposite trend is observed for the bandwidth, as a local maximum of 4.6 nm is obtained for 4 layers. However, if the time-bandwidth product (TBP) is considered, all SA samples generate pulses within the same trend in the EDFL. TBP refers to dispersion and chirp parameters from the laser cavity, and shows how far from the transform-limited value the pulse duration is. In fact, since the fiber laser system overall conditions change from sample to sample, the TBP seems to be the best parameter to compare the results among different number of graphene layers. Additionally, the peak in the spectrum for the graphene SA with $N = 1$ is localized in a different position as compared to the peak position for $N = 2\sim 7$, indicating that different types of solitonic pulses are formed in those situations (refer to Appendix D for details on the spectral and pulse width measurements).

By increasing the number of layers of the saturable absorbers sample, the total linear absorption is increased at a rate of $\sim 2.15\%$ per layer. Since the ultrafast recovery time remains constant for all samples, the main modification caused by the increasing number of layers is a change in the linear absorption profile of the SA, thus changing the temporal window for pulse formation [22,23]. As the number of layers increases, the optimal linear absorption is reached, and minimal TBP is obtained, for this laser cavity it was found that the best linear absorption level for generating the smallest TBP with stacked graphene monolayers is approximately 8.6% (4 layers). For higher number of layers, the oscillating bandwidth decreases, broadening the pulse temporal profile. Similar results have been demonstrated for carbon nanotubes saturable absorbers [24]. It is interesting to note that there is a difference of 4 to 6 orders of magnitude in the sample thickness from graphene to carbon nanotubes saturable absorbers, making this an important evidence that laser cavity parameters play a central role on pulse formation.

Our samples presented intracavity saturation intensities in the order of ~ 100 MW/cm², which is consistent with previously published results for graphene at 1550 nm [12,25,26].

5. Conclusions

In conclusion, stacked CVD graphene monolayer samples with 1 to 7 layers were fabricated. The samples were characterized by transient absorption experiments revealing that in the stacking process each monolayer is isolated from its neighbor layers. For all samples, in the absorption saturation regime, the carrier relaxation lifetime is 1 ps, independent of the number of monolayers. The stacked graphene monolayer samples were used as saturable absorbers in an EDFL cavity leading to the generation of pulses with duration ranging from 0.60 ps (1 layers) to 1.17 ps (7 layers), mainly determined by the saturable absorber's linear absorption. Our results show that with the SA with shortest pulse duration is the sample with single graphene monolayer. However, the overall minima for the time-bandwidth product is

obtained for SA with 4 layers, meaning that at this optical absorption level, the generated pulse is the closest to the transform-limited pulse width value. These results show that it is possible to maintain graphene SA samples ultrafast electron response while changing and controlling its optical properties, and use these SA samples to control EDFL performance.

Appendices

Appendix A: Optical and Raman characterization of stacked graphene monolayer samples

Linear optical characterization, atomic force microscopy and Raman spectroscopy were performed, and results are shown in Fig. 4. From Fig. 4(a), we observe the optical absorption scales linearly with the number of layers at a rate of $2.15 \pm 0.02\%$ per layer. Figure 4(b) shows the RMS roughness of final samples on top of glass substrate, measured in tapping-air mode over an area of $5 \times 5 \mu\text{m}^2$. Figure 4(c) shows that, for monolayer graphene, defect-related D band is practically absent, and the measured intensity ratio between G and 2D bands is $I(\text{G})/I(2\text{D}) \sim 0.25$.

In Fig. 4(d), the ratio between D and G bands intensities, $I(\text{D})/I(\text{G})$, is significantly small and kept almost constant for increasing number of layers, with maximum ratio of $I(\text{D})/I(\text{G}) \sim 0.042$ for 5 layers. Figure 4(e) shows that the intensity ratio $I(\text{G})/I(2\text{D})$ increases for a higher number of stacked layers, instead of remaining constant at the value of 0.25 for graphene monolayer. Since G band arises from a linear scattering process, its intensity should increase for an increasing number of layers, having contributions from individual layers. Figure 4(f) shows that the 2D band linewidth increases from $\sim 30 \text{ cm}^{-1}$ to $\sim 50 \text{ cm}^{-1}$, which is in agreement with [16] for weakly-coupled graphene monolayers.

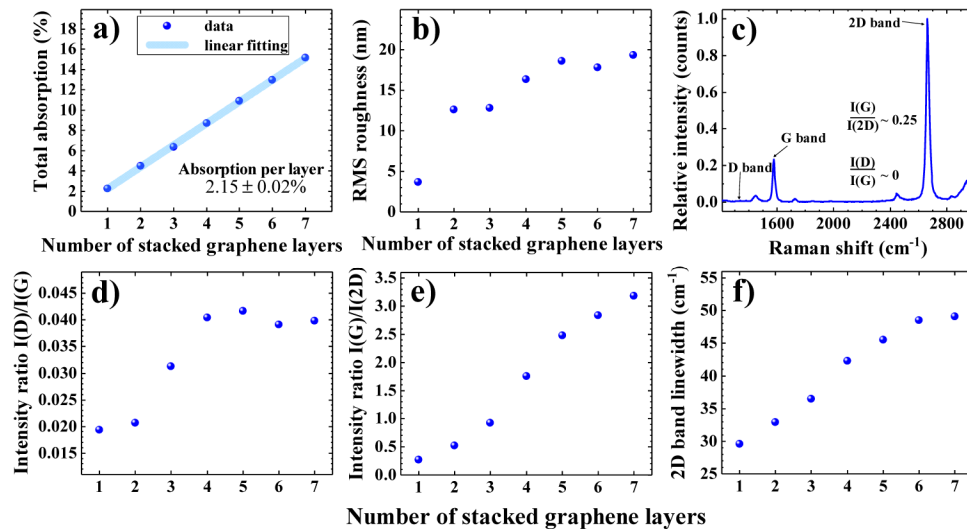


Fig. 4. (a) Linear optical absorption of the stacked CVD graphene monolayer samples at 1550 nm; (b) RMS roughness; (c) Raman spectrum of the transferred graphene monolayer sample; Raman spectroscopy analysis for samples with 1 to 7 stacked layers: (d) intensity ratio between D and G bands, (e) intensity ratio between G and 2D bands, and (f) 2D band linewidth.

Appendix B: Ultrafast spectroscopy characterization

The setup for the pump-probe experiment is shown in Fig. 5. From the optical parametric amplifier (OPA) are obtained both the intense pump (at 800 nm) and weak probe (at 1550 nm) beams.

The effects in stacked graphene monolayers are observed via changes in probe pulse transmittance, after sample is excited by pump pulse. By using a delay stage in the pump's

optical path, it is possible to control the relative arrival time between the earliest pump excitation and the probe pulse. Thus, the recovery of probe absorption, as a result of the relaxation of initial excited electrons, can be observed as a function of the delay time. The pump laser is chopped at 500 Hz, while the probe one is chopped at 357 Hz. The pump-and-probe signal (ΔT) is obtained by detecting the probe laser and measuring its electrical signal in a lock-in amplifier at the sum frequency. The spatial overlapping of the pulses was verified by directly observing them in a CCD camera at the sample position. The spot sizes of both lasers were maintained constants throughout the experiment. Further signal-to-noise improvement was reached using a spatial filter (pinhole) and a longpass filter (LPF) in the probe optical path before its detection.

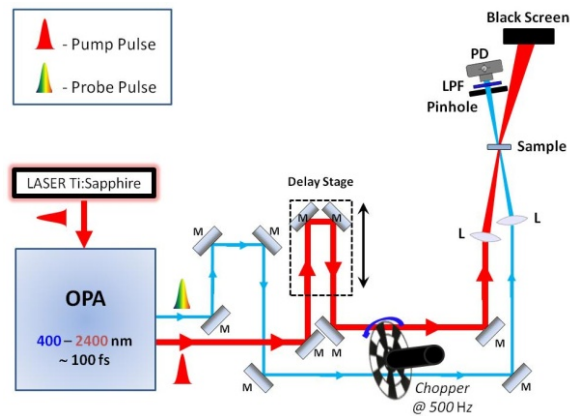


Fig. 5. Pump-and-probe experimental setup. OPA = optical parametric amplifier, M = mirror, L = lens, LPF = longpass filter, PD = photodetector.

Appendix C: Erbium-doped fiber laser setup

The fiber laser cavity used in this work is shown in Fig. 6. It has a 15 cm long highly-doped Erbium fiber as gain medium (66 dB/m @ 1550 nm, $D = -16$ ps/km/nm), pumped by a counter-propagating 980 nm diode laser ($P_{\text{pump(max)}} = 300$ mW). An integrated 980nm/1550nm pump-signal combiner and a 60-dB signal isolator is used to connect the pump laser to the gain fiber and to ensure unidirectional laser propagation.

Furthermore, a polarization controller is used to fine-tune the intracavity polarization state, and a 27% output coupler is used to extract the laser signal. The remainder of the cavity is made of 4.5 m of standard single mode fiber ($D = 17$ ps/km/nm). The fiber laser cavity has a total length of 4.95 m (fundamental repetition rate = 60.6 MHz), a total accumulated dispersion of +72.3 fs/nm and an average dispersion coefficient of +14.6 ps/km/nm, appropriate values for soliton pulses generation.

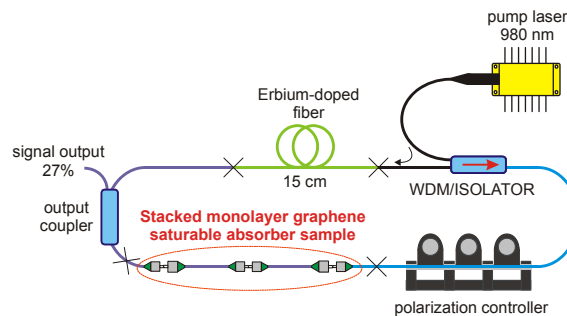


Fig. 6. Erbium-doped fiber laser cavity experimental setup.

Appendix D: Spectral measurements

Figure 7 shows the spectral measurements for graphene SA with 1 to 7 layers, along with an analysis of the central peak position for the soliton pulses. Fitting parameters are presented in Table 1. Additionally, the autocorrelation trace for samples with $N=1$ (minimum pulse duration obtained) and $N=4$ (local minimum pulse duration and absolute TBP minimum) are shown in Fig. 8.

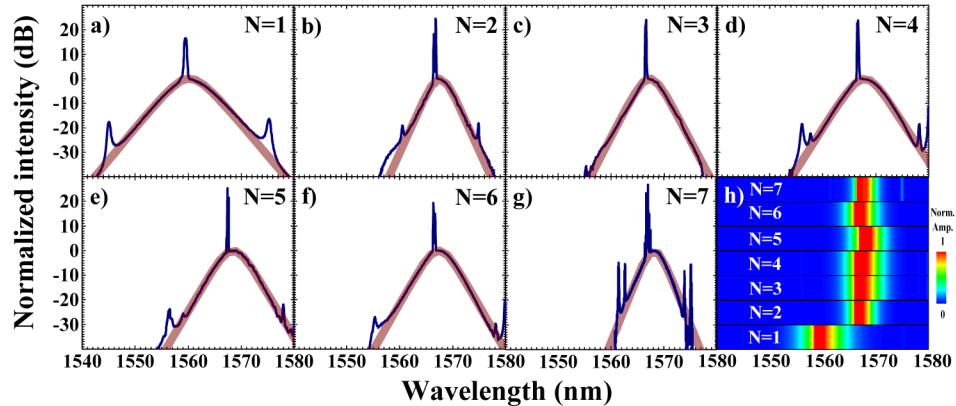


Fig. 7. (a)-(g) EDFL output spectra for $N = 1$ to $N = 7$. The thin blue line is the experimental data and the thick dark red line is the soliton-like ($\text{sech}^2(\omega)$) fitting. All spectra are amplitude normalized to the spectral peak power of the soliton pulse (excluding CW and side peak components). (h) The contour plot shows that the soliton for $N = 1$ has its peak centered at 1560 nm, while soliton spectra for $N = 2$ to $N = 7$ are red-shifted towards 1568 nm.

Table 1. Fitting parameters for all spectra from $N = 1$ to $N = 7$.

Number of layers	Central wavelength (nm)	Bandwidth (nm)
1	1560.3	6.00
2	1567.6	3.20
3	1567.3	3.75
4	1567.9	4.60
5	1568.5	4.25
6	1567.4	4.10
7	1568.2	2.90

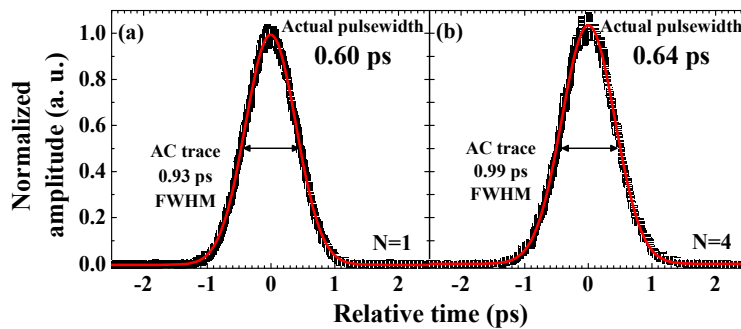


Fig. 8. Autocorrelation trace for output pulses with stacked graphene monolayer saturable absorbers with (a) $N = 1$ and (b) $N = 4$. The open dots are experimental data and the full red lines are $\text{sech}^2(\tau)$ fittings. The soliton form factor for actual pulse width is 0.648.

Funding

São Paulo Research Foundation (FAPESP) (Grant numbers 2010/19085-8, 2012/07678-0, 2012/50259-8, and 2013/16911-2).

Acknowledgment

J.A.C thanks CAPES for the financial support.